# 2D MODELLING AND ASSESSMENT OF DIVERTOR PERFORMANCE FOR ITER

A. S. Kukushkin, H. D. Pacher[1], D. P. Coster[2], G. Janeschitz, A. Loarte[1], D. Reiter[3], M. Rensink[4], T. Rognlien[4], R. Schneider[2], N. Asakura[5], S. Davies[6], K. Itami[5], B. LaBombard[7], B. Lipschultz[7], R. Monk[6], G. D. Porter[4]
ITER Joint Central Team, Garching JWS, Garching, Germany
[1] The NET Team, c/o Max-Planck Institut für Plasmaphysik, Garching, Germany
[2] Max-Planck Institut für Plasmaphysik, Garching, Germany
[3] FZ Jülich, Jülich, Germany
[4] Lawrence Livermore National Laboratory, Livermore, USA
[5] JAERI, Naka, Japan
[6] JET Joint Undertaking, Abingdon, UK
[7] PSFC MIT, Cambridge, USA

**Abstract**
The results of the ITER divertor modelling performed during the EDA are summarised in the paper. Studies on the operating window and optimisation of the divertor geometry are presented together with preliminary results on the start-up limiter performance. The issue of model validation against the experimental data which is crucial for extrapolation to ITER is also addressed.

## 1. INTRODUCTION

The present paper summarises the design studies [1–4] done for the ITER EDA divertor using the B2-Eirene code and shows results from application of the same model to actual discharges from the multi-machine data base.

## 2. MODEL VALIDATION

Model validation using the "ITER edge profile database" has recently been started [5]. This database contains data provided by Alcator C-mod, DIII-D, JET and JT-60U. First simulations without impurities have been carried out for all devices, and simulations with impurities (carbon, physical sputtering plus 1% yield roughly simulating chemical sputtering) have been performed so far only for JT-60U in L-mode. A recycling coefficient of 1 for all surfaces and anomalous perpendicular transport constant in space for particles and energy are assumed here.

### 2.1. Ohmic and L-mode discharges

JET and JT-60U discharges having similar main plasma parameters (2 MA L-mode density scans with ~4 MW of additional heating) can be modelled with similar input parameters. JT-60U plasmas with impurities and JET experiments in a similar regime are satisfactorily modelled with the same values of the transport coefficients ($D = 0.15\ m^2s^{-1}$, $\chi = 5.0\ m^2s^{-1}$). In both EDGE2D and B2-EIRENE simulations of JET, the outer divertor agrees better, i.e. it is in the high recycling regime in both experiment and the simulations, whereas the inner divertor is more detached in the experiment than in the codes. JT-60U impurity radiation levels are well reproduced by the carbon production assumption above over the whole density scan. Impurities are needed to describe properly the sudden approach to detachment at the measured separatrix density and the measured radiated power fraction. The $Z_{eff}$ found by the code falls from 2.2 to 1.2 as $n$ is raised, whereas it remains constant around 2 in the experiment (see Ref. [5] and references therein).

In contrast, Alcator C-mod mid-plane and divertor profiles in equivalent Ohmic regimes can be modelled only by using input values very different from those for JET and JT-60U, i.e. $D = 0.2\ m^2s^{-1}$, $\chi = 0.04\ m^2s^{-1}$. A strong particle sink at the divertor (modelled by taking $R = 0.8$ there) must be assumed, requiring also a strong particle source in the core plasma and leading to a much stronger normalised particle flow (30% vs. less than 10%) and convective energy flow (90% vs. 10%) than in the other devices and ITER. In the current modelling, the sink provided by realistic bypasses (restoring R=1) is too small and the deduced core particle source is also too small and does not correspond to the (higher) measured core $H_\alpha$.

## 2.2. H-mode discharges

Low density ELMy H-modes between ELMs are modelled for similar plasma states in JET and DIII-D. B2-EIRENE and EDGE2D results for JET are similar: divertor ion flux and $T_e$ and SOL power flow can only be reproduced using very low diffusion coefficients and a large ratio of ion to electron power flow. This occurs also in B2-EIRENE simulations of DIII-D, for which power profiles can be compared with infrared measurements. $P_i/P_e$ here is 4.0 and diffusivities are similar to those used for JET, $D_\perp = 0.01\ m^2s^{-1}$, $\chi_{\perp e}= 0.70\ m^2s^{-1}$, $\chi_{\perp i} = 0.35\ m^2s^{-1}$. The very peaked divertor electron temperature profile and the upstream electron temperature and density profiles are all reproduced (Fig. 1). The ion temperature in the SOL is underestimated here. Therefore, if charge-exchange measurements are representative of the Maxwellian ions, then the parallel ion heat flux would be flux limited in the experiment, whereas no ion flux limit was imposed in these simulations.

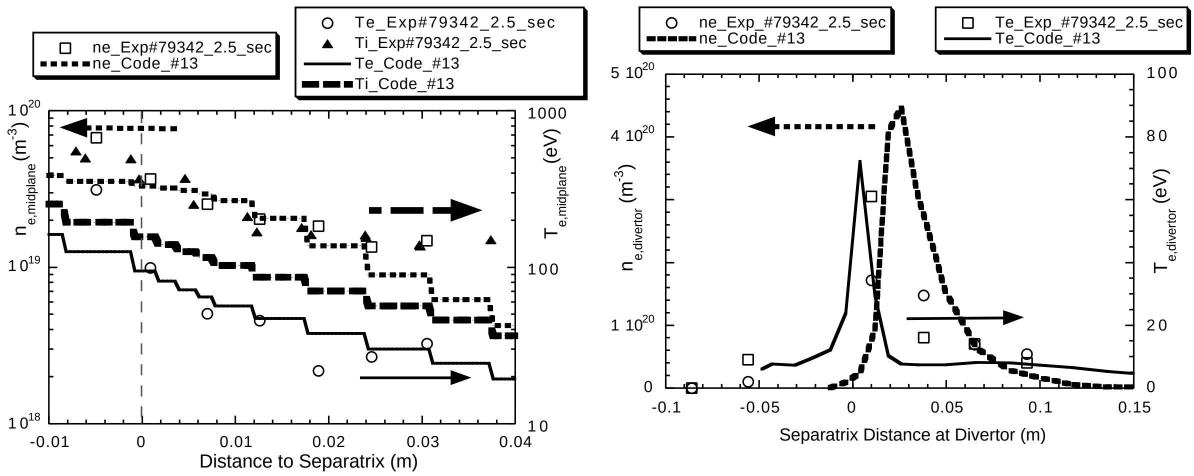


*FIG. 1. Radial profiles of $T_e$, $T_i$, and n in the mid-plane SOL (left) and of $T_e$ and n at the target (right) for a DIII-D low density ELMy H-mode discharge and B2-EIRENE simulation [5]*

## 3. OPERATING WINDOW FOR THE ITER DIVERTOR

The principal parameters limiting divertor operation in ITER are the peak power loading of the target which should be below 10 MW/m$^2$ and the helium pressure in the private-flux region (PFR) which should be sufficient to exhaust 2 Pa-m$^3$/s of helium [4]. Compatibility with the core plasma requires that the separatrix density upstream $n_s$ be (3 to 4)$\times10^{19}$m$^{-3}$ and $Z_{eff}$ at the core-edge interface (CEI) be less than 1.8. The edge plasma density, cross-field transport, input power, particle throughput, and neon seeding level have been varied to explore the operating window of the ITER divertor. In these calculations, the plasma consists of D-T, He, C, and Ne ions and their transport is described self-consistently. He and Ne are introduced through their concentration at the CEI, and physical and chemical (Y=0.01) sputtering at the target plates provide the C source.

It is found that under our standard transport assumptions ($\chi_\perp = 1\ m^2/s$ , $D_\perp = 0.3\ m^2/s$), the peak power loading is acceptable over practically the whole required density range (Fig. 2). Reduction of $\chi_\perp$ and $D_\perp$ by a factor of 2 leads to a considerable increase of the power loading, but this can be compensated by a reduction of the input power by 25% (increasing radiation from the "mantle" [1]).

The calculated DT and helium pressures are shown in Fig. 3 (calculated at approximately constant pumping speed except for the two points marked "low core flux"). For a typical point in the middle of the range, at $n_s$=0.331 $10^{20}$ m$^{-3}$ the pressure shown corresponds to a DT throughput of 219 Pa-m$^3$/s at a pumping speed $S_{DT}$=130 m$^3$/s. The helium throughput is 3.4 Pa-m$^3$/s at $S_{He}$=106 m$^3$/s (i.e. 80% of $S_{DT}$). There is therefore a margin of about 1.7 in helium pumping with respect to the required 2 Pa-m$^3$/s at 1.5 GW fusion power, or, conversely, a helium fraction at the core-edge interface of 6% would be expected at the required helium throughput rather than the 10% used in the calculation. When pumping speed and DT throughput are varied simultaneously keeping the upstream density constant, it is found that the ratio of divertor pressure to upstream density varies weakly, and as a result the upstream helium fraction varies strongly with DT throughput. It is concluded that DT pumping speeds larger than 120 m$^3$/s and

DT throughputs larger than 190 Pa-m$^3$/s are required to maintain the upstream helium fraction below 10% for ITER conditions.

The results indicate that the peak heat loads decrease only slowly as the seeded neon increases ($Z_{eff}$ variation in Fig. 2). This is apparently related to the constant chemical sputtering yield used in the calculations, because an increase of the neon radiation reduces the hydrogen flux which then reduces the carbon release from the target. Impurity seeding therefore can make up the radiation if the carbon source were smaller, but does not modify the ITER operating point.

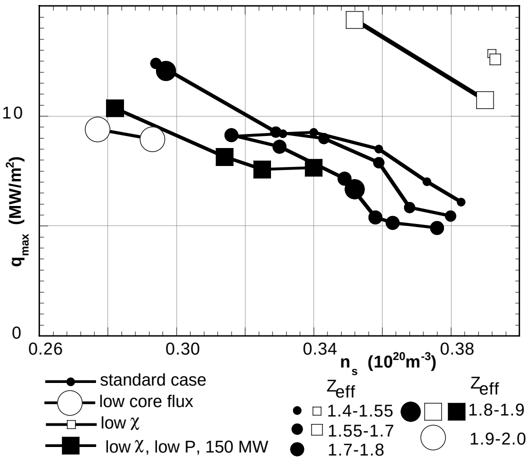


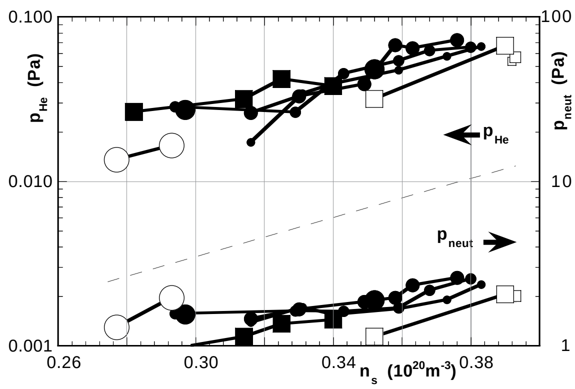


*FIG. 2 (left). Peak power load at the divertor target vs. upstream density $n_s$ for "standard case" (solid circles), for lower $\chi$ and D (hollow squares), for simultaneous lower $\chi$ and D and lower SOL power (solid squares) and for lower throughput (hollow circles), all for reference divertor geometry. Various $Z_{eff}$ (obtained by varying the neon fraction) are indicated by symbol size.*

*FIG. 3 (right). Average helium partial pressure and total neutral pressure at plasma-PFR interface vs. $n_s$ for reference divertor geometry. Legend see Fig. 2.*

Start-up conditions in ITER have been modelled with the UEDGE code for a toroidally symmetric limiter inserted to a normalised flux of 0.935 with the core boundary located at 0.87. Here the CEI density is set to $5{\cdot}10^{19}$ m$^{-3}$, and $\chi_\perp = 0.5$ m$^2$/s and $D_\perp = 0.33$ m$^2$/s are used. Variation of the input power from 6 MW to 30 MW and of the limiter angle to the magnetic surfaces from normal to almost tangential (3˚) reveals no evidence of significant particle recycling. The peak heat flux scales almost linearly with discharge power and inversely with the wetted area, being 8 MW/m$^2$ for 20 MW on the normal limiter. Simple estimates of the power load based on the SOL width [6] should therefore remain valid.

## 4. GEOMETRY OPTIMISATION

Three studies aimed at the optimisation of the divertor geometry are reported here: an analysis of the importance of the “wings” in the PFR [7], a determination of the optimum size of the shielding structure in the PFR (the so-called “dome”), and a comparison of divertors of different length.

It is found that the presence of “wings” along the divertor channels in the private-flux region is not expected to have a large influence on the divertor parameters because only a small fraction of the parallel momentum (less than 10%) is transferred to them by the neutrals [3].

In order to see the effect of the dome, four series of calculations were done for different dome shapes, ranging from the open PFR without dome to a slot-like divertor whose dome length is 80% of the divertor length [4]. It is found that a much longer dome would impede the transition to the partially attached state and therefore would yield higher heat loads, whereas removal of the dome would degrade helium pumping by a factor of 2. It is therefore recommended to retain the present dome.

The effect of reducing the divertor length was studied using the ITER divertor and divertors having 0.75 and 0.5 of its length [4]. In order to separate the effect of the divertor length from that of the magnetic flux expansion near the x-point, the geometry of the targets was adjusted to keep the same surface area interacting with the plasma – that is, the same angle of the field line to the target – at least in the vicinity of the separatrix strike-points. Fig. 4 shows the cumulative integral of the power radiated in the divertors for these three options. Reduction of the divertor length squeezes the radiation region towards the targets and increases the radiation load. The increase of the peak power loading is considerable, Fig. 5, but a further optimisation of the divertor geometry or impurity composition, or a minor reduction of the input power could bring it below 10 $MW/m^2$. The margin for helium pumping remains the same within 20%.

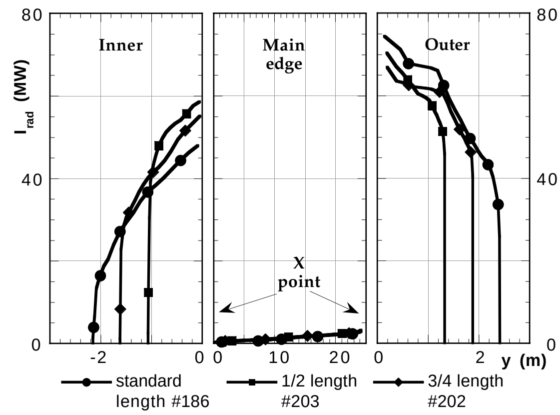


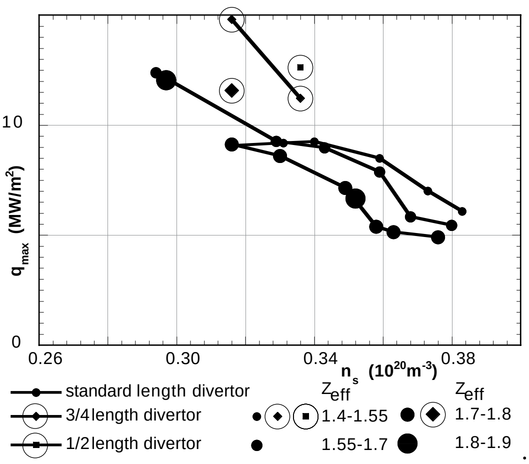


*FIG. 4 (left). Cumulative integral of radiation power density (already integrated radially) in poloidal direction vs. distance from target to X-point (inner divertor and PFR, left pane), from X-point to X-point (edge plasma and SOL, central pane) and from X-point to target (outer divertor and PFR, right pane), for standard, three-quarter, and half-length divertors.*

*FIG. 5 (right). Peak power as in Fig. 2 but for standard, three-quarter, and half-length divertors*

## 5. CONCLUSIONS

The 2D model used for ITER divertor modelling reproduces a number of experimentally observed features of discharges in the multi-machine database. First results for startup operation of ITER show that significant particle recyling does not occur at the limiter and that therefore simple estimates of the limiter power load can be used.

Application of the 2D model to the ITER divertor yields the conclusion that the ITER divertor provides acceptable power loads and helium pumping for the expected mid-plane separatrix densities and radial transport coefficients. It can also accommodate low $\chi_\perp$ and low $n_s$ with a modest SOL power reduction and an acceptable operating window for heat load and He pumping. The "wing" structures are not required. Modifications desirable for other reasons (shorter divertor, dome removal, reduced DT throughput) reduce this window.

## REFERENCES

[1] KUKUSHKIN, A., PACHER, H. D., ABRAMOV, V., *et al.* , Fusion Energy (Proc. 16th IAEA Fusion Energy Conference, Montreal, 1996), Vol. 2, IAEA, Vienna (1997) 987–993.

[2] KUKUSHKIN, A., PACHER, H. D., COSTER, D., *et al.*,, Eur. Conf. Abstracts (Proc. 24th EPS Conference on Controlled Fusion and Plasma Physics, Berchtesgaden, 1997), Vol. 21, Part III (Schittenhelm, M., Ed.), The European Phys. Soc. (1997) 1001–1004.

[3] KUKUSHKIN, A., PACHER, H. D., COSTER, D., *et al.*, , Contributions to Plasma Physics, **38** (1998) 20–25.

[4] PACHER, H. D., KUKUSHKIN, A. S., COSTER, D. P., *et al.*, "Operating window for high divertor radiation in ITER", Proc. 13th PSI Conference, San Diego, May 1998 *(to be published in J. Nucl. Mater.).*

[5] LOARTE, A., KUKUSHKIN, A., PACHER, H., "Comparison of B2-EIRENE calculations with multi-machine experimental measurements", Proc. 13th PSI Conference, San Diego, May 1998 *(to be published in J. Nucl. Mater.).*

[6] PACHER, H. D., NET Internal Note N/I/3340/4/A, "Power Loads on optimised port limiters", Nov. 1997

[7] JANESCHITZ, G., PACHER, H. D., FEDERICI, G., *et al.* , Fusion Energy (Proc. 16th IAEA Fusion Energy Conference, Montreal, 1996), Vol. 2, IAEA, Vienna (1997) 755–767.